J Mater Sci: Mater Med (2010) 21:1937–1947
DOI 10.1007/s10856-010-4061-1

Initial biocompatibility and enhanced osteoblast response of Si doping in a porous BCP bone graft substitute

In-Seon Byun · Swapan Kumar Sarkar · M. Anirban Jyoti · Young-Ki Min · Hyung-Seok Seo · Byong-Taek Lee · Ho-Yeon Song

Received: 14 December 2009 / Accepted: 15 March 2010 / Published online: 2 April 2010

Abstract Granular shape biphasic calcium phosphate (BCP) bone grafts with and without doping of silicon cations were evaluated in regards to biocompatibility and MG-63 cellular response. To do this we studied Cellular cytotoxicity, cellular adhesion and spreading behavior and cellular differentiation with alizarin red S staining. Gene expression in MG-63 cells on the implanted bone substitutes was also examined at different time points using RT-PCR. In comparison, the Si-doped BCP granule showed more cellular viability than the BCP granule without doping in MTT assay. Moreover, cell proliferation was much higher when Si doping was employed. The cells grown on the silicon-doped BCP substitutes had more active filopodial growth with cytoplasmic webbing that proceeded to the flattening stage, which was indicative of well cellular adhesion. When these cells were exposed to Si-doped BCP granules for 14 days, well differentiated MG-63 cells were observed. Osteonectin and osteopontin genes were highly expressed in the late stage of differentiation (14 days), whereas collagen type I mRNA were found to be highly expressed during the early stage (day 3). These combined results of this study demonstrate that silicon-doped BCP enhanced osteoblast attachment/spreading, proliferation, differentiation and gene expression.

I.-S. Byun · M. Anirban Jyoti · Y.-K. Min · H.-Y. Song (✉)
Department of Immunology, School of Medicine, Soonchunhyang University, Cheonan, Chungnum 330-090, South Korea
e-mail: songmic@sch.ac.kr

S. K. Sarkar · B.-T. Lee
Department of Biomedical Engineering and Materials, School of Medicine, Soonchunhyang University, Cheonan, Chungnum 330-090, South Korea

H.-S. Seo
Department of Health Science, Konyang University, Nonsan, Chungnum 320-711, South Korea

1 Introduction

Bone tumor, osteolysis, osteoporosis or accidental/surgical trauma might cause severe bone loss which should be repaired or replaced. To replace damaged hard tissue or to aid in the replacement of hard tissue, implants, either obtained from different sites of the patients' body (autotransplantation) or donors (allotransplantation or xenotransplantation), that play a supporting mechanical role must be developed. There are many shortcomings associated with autografts, homografts or xenografts including availability, tissue rejections, requirements for immunosuppressant drugs, viral or prion contaminations, and ethical problems [1]. Therefore, there is an increasing demand to develop novel biomaterials that can speed up the natural healing process of disordered skeletal tissue after replacement surgery [2]. However, the high failure rates of the implants have motivated biomaterial scientists to synthesize biomaterials that can effectively mimic natural bone [3]. To solve the problems associated with autotransplants, allotransplants, and xenotransplants, researchers are developing bone substitutes that are based on calcium phosphate ceramics, such as HAp (hydroxyapatite), α/β-TCP (alpha/beta-tricalcium phosphate) and BCP (biphasic calcium phosphate). These materials are the main constituents of natural bone which result in limiting inflammation, body rejection and any other complications associated with auto, allo and xenotransplants that negatively impact implantation surgery. Since 70% of natural bone is comprised of minerals, such as naturally occurring hydroxyapatite (HAp), a large effort has been directed at using HAp to

develop artificial skeletal tissues [4–6]. Although HAp is biocompatible, some studies have shown that stoichiometric HAp has limitations due to low resorbability which may cause loosening of the implant, disintegration or poor handling characteristics [7, 8]. Moreover, its limited ability to form a stable interface with bone has further impaired the use of HAp in bond replacement applications [9]. As an osteoconductive ceramic, β-Tricalcium phosphate (β-TCP) is another potential candidate material for bone replacement applications. However, this material also has limitation, such as -high resorption rate and low strength and mechanical properties. Therefore, the compatibility of bi-phasic calcium phosphate (BCP), which consists of both HAp and β-TCP, has been investigated as a potentially ideal biomaterial for bone replacement applications. BCP ceramics are currently used in orthopedics and dentistry because of their strong mechanical strength and biodegradability [10, 11]. This composite material has the distinct advantage in that the disadvantages of using HAp and β-TCP by themselves is mitigated when both are used together [12, 13].

In the inorganic part of bone mineral various ionic substitutions have been identified. Among them, carbonate ions have been found at a concentration of 8 wt%. Other ionic substitutions occur in trace amounts such as Na, Mg, K, Sr, Zn, Ba, Cu, Al, Fe, F, Cl and silicon (Si) [14]. These substitutions play important roles between Ca–P implant and mineral bone by influencing the morphology, surface chemistry and solubility of the material. Among these substitute ions, Si has been shown to be one of the most essential elements for bone cell development [15–22]. Bone remodeling is controlled by a balanced activity between osteoblast (bone formation) and osteoclast (bone resorption). The presence of silicon increases the number of osteoblasts and cell activity [15]. Silicon plays important roles in bone during the early stage of bone formation and the calcification process [16–19]. It also up-regulates the expression of certain genes such as BMP-2 and collagen [20–22]. Several researches have been performed on silicon substitution of ceramics. Calcium silicate ceramics have been shown to be bioactive, degradable, and biocompatible. Especially, beta-calcium silicate (β-$CaSiO_3$) increases cell attachment and proliferation rates compared to β-TCP ceramics, which is commonly used in dental and orthopedic implants [23]. Silicate-substituted hydroxyapatite scaffolds improve the bone healing response [24–26]. Previous studies reported that increased dissolution rate due to Si substitution might be the reason for increased osteoactivity and bone cell regeneration [27, 28].

Also surface morphology and topography of a ceramic material have great influences to overall biocompatibility but they differ due to different surface chemistry. Si incorporation thereby according to Balas et al. [29], acts like an enhancer for bone cells to differentiate and proliferate as the material surface chemistry has been altered from its bulk composition by Si substitution.

In this study, we prepared granule type silicon-doped porous BCP bone graft substitutes using the fibrous monolithic (FM) process, and evaluated the biocompatibility of the substitute. The cell adhesion/spreading process, proliferation, growth behavior and differentiation of MG-63 human osteoblast-like cells were examined on these bone substitutes. The expression of osteoblast specific genes was investigated during the differentiation period.

2 Experimental procedures

2.1 Powder synthesis

The BCP powder was by a wet chemical process by the help of ultrasonic energy. Both $Ca(NO_3)\cdot 4H_2O$ and $(NH_4)_2HPO_4$ were separately dissolved in de-ionized water and mixed in an ultrasonic bath. The reactant was weighed such that the Ca/P ratio of the powder was 1.585, which resulted in a theoretical HAp/TCP ratio of 1. Sodium Silicate solution was used as precursor to incorporate the Si dopant. Si content was selected so that the final content of this material in the BCP would be 1.5% by weight. NH_4OH solution was slowly added to the bath to raise the pH of the solution to 10.5. Continuous ultrasonic exposure was carried out for 4 h and then the suspension was transferred to a beaker washed for 4 times with de-ionized water and filtered. The powder was dried and then calcined at 750°C for 1 h. A silicon content of 1.5% by weight of the BCP powder was selected.

2.2 Fabrication of porous granule and characterization

The calcined BCP powders were used to fabricate the porous granules by the extrusion process as described elsewhere [30–32]. Carbon was used as the fugitive pore forming agent, which is removed completely at one stage. The details of the fabrication and subsequent characterization are under the submission procedure separately. In short, the BCP powders and Carbon were mixed separately with the polymer of vinyl acetate (EVA) (ELVAX 210 and 250, Dupont, USA) and stearic acid ($CH_3(CH_2)_{16}COOH$, Daejung Chemicals & Metals Co., Korea) by a shear mixing machine(C.W. Brabender Instruments, Shina platech Co., Hwaseong Gyeong-Gi-Do, Korea).

The polymer mixed thermoplastic materials were made to form a core/shell cylindrical feed role with 50:50 volume ratios where the core was carbon. The core shell assembly was placed into a steel die and extrusion was carried out at 120°C to make two filaments that were 1 mm in diameter.

To remove the EVA binder, a burning-out process was carried out at 700°C for 2 h in a N_2 atmosphere and to drive the pore forming carbon they were again burnt out at 1000°C. Finally, a pressure-less sintering process was carried out at a temperature of 1300°C for 2 h in an air atmosphere. The microstructure morphology and the composition of the bone substitute were determined by SEM and ICP-AES analysis, respectively.

2.3 Cell culture and differentiation

In this study, two cell lines, Human fibroblast-like cells, L-929 derived from mouse fibroblasts, and human osteoblast-like cells, MG-63 derived from human osteosarcoma, were used to assess cell viability, growth behavior (adhesion/spreading) and differentiation of cells on the bone substitutes. Both cells were obtained from KCLB (Korean Cell Line Bank). L-929 cells were maintained and cultured with PRMI media (RPMI-1640; HyClone, Logan, UT) and MG-63 with DMEM (Dulbecco's Modification of Eagle's MEM, HyClone, Logan, UT). Both media were further supplemented with 10% heat inactivated fetal bovine serum(FBS, Gibco), 2 mM L-glutamine(Sigma), 100 U/ml penicillin(Sigma), 100 μg/ml streptomycin (Sigma) and 0.25 μg/ml fungizone (Bio-Whittaker), and placed in an incubator containing 5% CO_2 at 37°C. During sub-culturing EDTA-Tryptophan was used to detach the cells from the T-75 flask and cells were counted under a LM using Typan blue stain and haemocytometer.

2.4 Cell adhesion/spreading and growth behavior

MG-63 cells (1×10^3 cells/ml) were seeded on the top surfaces of the granules in a 96-well plate. After 20 min the cells were fixed to examine the adhesion/spreading behavior by scanning electron microscopy (SEM) (JSM-5410LV JEOL). In addition, the growth behaviors of cells were observed after 7 days by SEM. For the SEM observation, the cells were fixed in 2% glutaraldehyde and dehydrated in ethanol (50–100%). The dehydrated cells were dried in hexamethyldisilazane (Sigma) and coated by gold sputtering.

2.5 MTT assay

Semiautomated MTT assay was used to determine the cytotoxicity against fibroblast-like L-929 cells and proliferation of osteoblast like MG-63 cells. The cytotoxicity or MTT (3-[4,5-dimethylthiazol-2-yl]-2,5-diphenyltetrazolium bromide) assay was employed to determine cell viability on the fabricated BCP granules [33]. The extraction method and procedures used in this assay were outlined in ISO 10993 [34]. In brief, after obtaining the extract solution for the IBS samples, they were diluted serially with media (25, 50 and 75%). 100% media and 100% extract solution were used as positive and negative control respectively. Then extract solution and control (1 ml) were added into 24 well plates which were previously sub-cultured with cells (10^4 cells/well). The plates were incubated for 72 h at 37°C. To quantify cell survival/proliferation at different dilutions, 100 μl MTT solutions (20 μg/100 ml) were added to each of the wells. Hence it should be noted that MTT assay is a colorimetric assay which measures the metabolic activity of viable cells. After addition, MTT solutions were dissolved into the media which created a yellowish color. The dissolved MTT was converted to insoluble purple formazan by dehydrogenase enzyme of the mitochondria which was the product of live cells only. The amount of oxidized MTT was measured by spectrophotometrically after the formazan was dissolved in DMSO (dimethyl sulfoxide). To get the best absorbance of dissolved formazan, the 24-well culture plates were incubated for 4 h and 1 ml of DMSO was added to each of the wells and the absorbance was quantified using an ELISA reader (EL, 312, Biokinetics reader, Bio-Tek instruments) at a wavelength of 595 nm.

2.6 RNA isolation and RT-PCR

The sample extracts were prepared by first incubating the sample in DMEM media at 37°C for 72 h in a shaking incubator with 100 rpm (orbital). MG-63 cells were incubated with the extract solutions of each sample for 3, 7, 14 days. Total RNA was extracted from the cells using the RNeasy kit (Qiagen Inc. Valencia, CA) according to the manufacturer's instructions. The RNA concentration was measured spectrophotometrically at 260 nm and its purity was determined by the ratio of absorbance at 260–280 nm and by agarose gel electrophoresis. RNA samples (1–2 μg) were reverse-transcribed to cDNA using M-MLV reverse transcriptase and oligo-dT. Three reaction steps were performed (30–40 cycles): I. Denaturation step at 94°C for 1 min, II. Annealing step at 55–65°C for 1 min, and III. Extension step at 72°C for 1 min. The primer pair sequences designed for this study were obtained from Primer 3 (http://frodo.wi.mit.edu/primer3/) shown in Table 1.

2.7 Statistical analysis

All statistical analyses were performed using SPSS (Statistical Package for the Social Sciences version 16, SPSS Inc., USA). Results are expressed as means ± standard error (SE). Student's *t*-test was used to compare among different treatment groups with significance assigned at $P < 0.05$.

Table 1 Primer sequences for RT-PCR

Gene	Forward primer	Reverse primer
Osteonectin	ACATGGGTGGACACGG	CCAACAGCCTAATGTGAA
Osteopontin	TGACCTCTGTGAAAACAGCGT	TGTACATTGTGAAGCTGTGAA
Collagen-1	TGGAGAGTACTGGATTGACC	AGTGGTAGGTGATGTTCTGG
GAPDH	CTGCACCACCAACTGCTTAG	AGGTCCACCACTGACACGTT

3 Results and discussion

3.1 Characterization of the porous granule type of BCP bone substitutes

Both optical and SEM images of the samples were acquired for the morphological investigation of the fabricated bone substitutes. The fabricated granular type Si-doped BCP bone substitutes showed no conspicuous differences in terms of the morphology of the surface-frames compared to that of the BCP bone substitutes without containing Si. The morphology of the fabricated bone substitutes provided much information related to the extent of biocompatibility of the samples used herein with the in vitro studies depending on the effect of Si doping in the bone substitutes. We have successfully shown that the granular type of silicon-doped BCP bone substitutes enhanced cell attachment, spreading, proliferation and differentiation.

Figure 1a and b shows the optical and SEM images of the sintered granular BCP bone substitutes with and without silicon doping. There was not any noticeable difference as the processing methods and parameters were similar, except the trace amount of Si doping during the synthesis period of BCP powders prior to the fabrication process. Both bone substitutes were cylindrical in shape and had a diameter of 1.0 mm. Each granule had a porous interior with seven channels extended through one end to another. The optical image in Fig. 1a shows the surface of the round face of the bone substitute. The channel openings were very rough and irregular. However, no severe processing defects, such as cracks and de-bonding were observed in the frame. The channel diameter was around 180 μm and the frame thickness was 80–120 μm. Figure 1c and e shows the SEM image of the dense frame region of the bone substitute for non-doped and Si-doped granules, respectively. The densification was nice and the grain size of the sintered material was around 4–8 μm in. This indicated that the particle had undergone a significant grain coarsening during fabrication since the BCP powders used had particle size of only 50 nm. The granules were through channeled (around 180 μm) and the frame was thin (around 80–120 μm). The relative density was 51.2 ± 2.1. As the granules were 1–1.5 mm in length, the cellular growth could be favored by reaching the adjacent porous granule and covering the channel surfaces. Thus the osteogenic cells can proliferate completely in the whole defect sites. This is the exact thing we expect from interconnected porosity, which is a very important factor for the osteointegration of the implant materials.

We also tested the compositional variations of the bone substitutes after fabrication by ICP method. Table 2 shows that the Si content of the final materials is 1.5% silicon. In a previous study, in vivo bioactivity was greatly increased with 1.5% SiHAp (silicate-substituted hydroxyapatite) [35]. Figure 1d and f shows SEM images of the inside surface of the channel for both of the granules. The inner surfaces of the channels were extremely rough and the roughness was bi modal. It is now well known that cellular attachment, adhesion, spreading, proliferation and differentiation can largely be affected by the biomaterial surface properties [36–40]. Bigerelle et al. [40] showed that cellular adhesion and proliferation of human osteoblast was largely affected by the roughness of the material surface (titanium and titanium-based alloys). High surface roughness increases the overall surface area that the implant has to interact with adjacent osteogenic cells in the bone microenvironment. The surfaces of both samples were extremely rough. This was a highly favorable feature since the rough surface makes it easier for proliferating cells to strongly attach within the pore surface and it can act as a mechanical support for further cell proliferation in multiple layers [36–40]. However, the study concerns that this roughness factor might have a contributory effect on the relative comparison of the doped and non-doped granules. But as it was mentioned earlier that the roughness was developed only because of the processing method and not related to the doping of Si, it has no variable effect on the cell proliferation behavior on these two kind of bone substitutes.

3.2 Cell cytotoxicity and proliferation

In this study, no cellular toxicity that could adversely affect cellular proliferation was observed due to the exposure of the Si-substituted BCP granules to the fibroblast-like L-929 cells (Fig. 2). Cellular cytotoxicity was determined using the MTT assay and the results are shown in Fig. 2. The results were expressed as a relative percentage of the

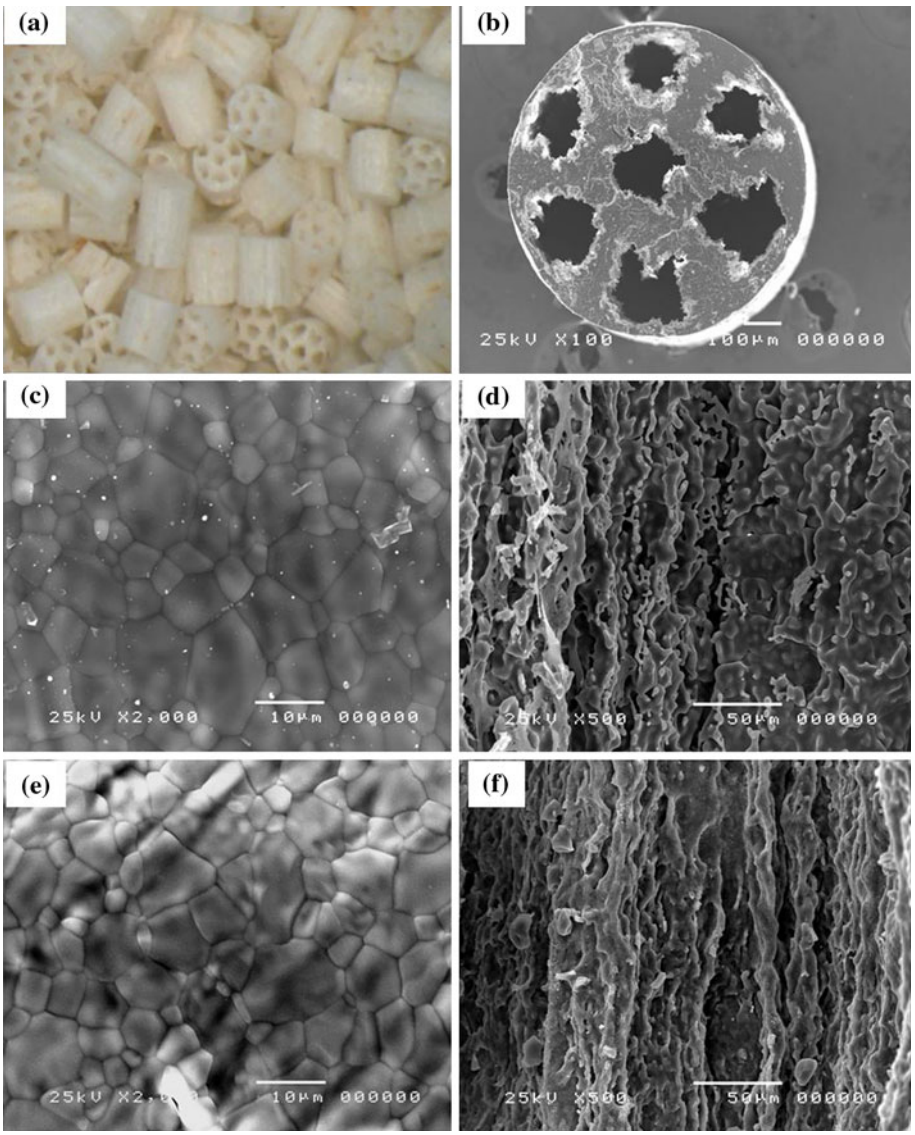

Fig. 1 **a** Optical microscopic and **b** SEM images of granular bone substitutes. **c**, **d** Frame and pore surface of the granular bone substitute without any doping. **e**, **f** Frame and pore surface of the granular bone substitute with 1.5% Si doping

Table 2 ICP results of BCP and Si-doped BCP powder

	Ca (%)	P (%)	Si (%)	Fe (mg/kg)
BCP	36.9	19.9	–	15.2
Si-doped BCP	36.0	20.0	1.5	12.4

absorbencies measured in the control and extract-treated cells. Survival rate of the cell was over 90% for both BCP and silicon-doped BCP bone substitutes. The relative viability of the silicon-doped BCP bone substitute was slightly higher than BCP.

Furthermore, an increased cellular proliferation was observed upon incubation of osteoblast like MG-63 cells with the substituted samples.

We also measured the cellular proliferation rate of MG-63 cells in diluted extract solutions of both Si-doped

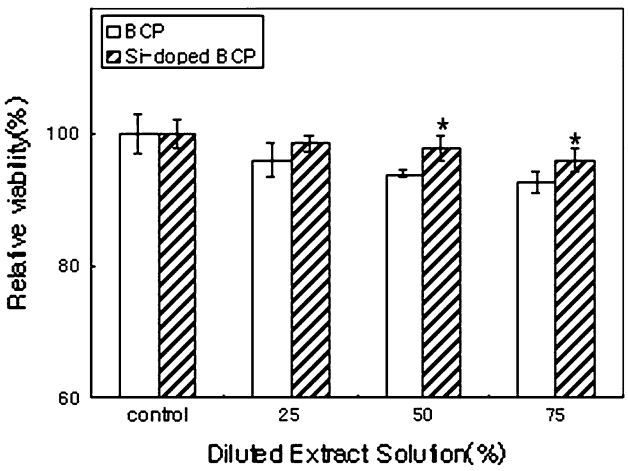

Fig. 2 Cell cytotoxicity of the diluted extract of the BCP and silicon-doped BCP bone graft substitutes against L929. * Denotes the significant value in the cell viable count ($P < 0.05$)

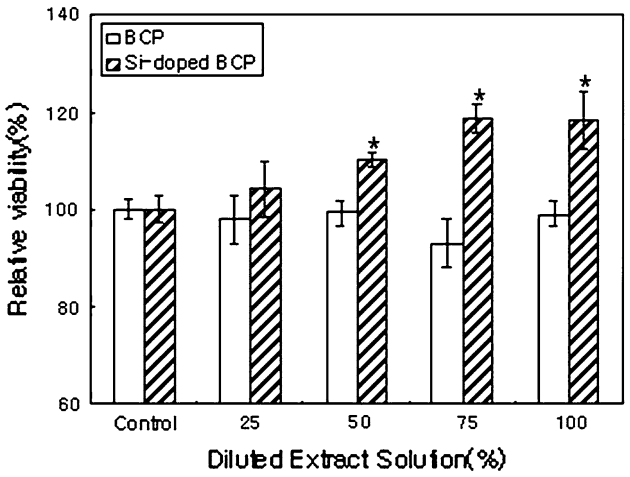

Fig. 3 MG-63 osteoblast-like cell proliferation in the extract solution of the BCP, Si-doped BCP bone substitute by MTT assay for 3 days of culture. * Denotes the significant value in the cell proliferation count ($P < 0.05$)

and non-doped bone substitutes. Silicon-doped porous BCP bone graft substitutes showed an enhanced MG-63 osteoblast-like cell proliferation, which was even better than that of the BCP bone graft substitutes (Fig. 3). Figure 3 shows that Si doping had a clear effect on cellular proliferation by increasing the cellular viability. This result is in agreement with previous findings by Xu et al. [41] where they showed that Si substitution in HA significantly increased cellular proliferation.

3.3 Cell adhesion/spreading and growth behavior

Trypsin harvested and washed cells were subjected to SEM images after 20 min of seeding on a culture dish and BCP granules with and without the Si dopant by using glutaraldehyde as a general fixation agent. The cellular adhesion and spreading processes of MG-63 osteoblast cells were observed by SEM. Figure 4 shows the SEM images of

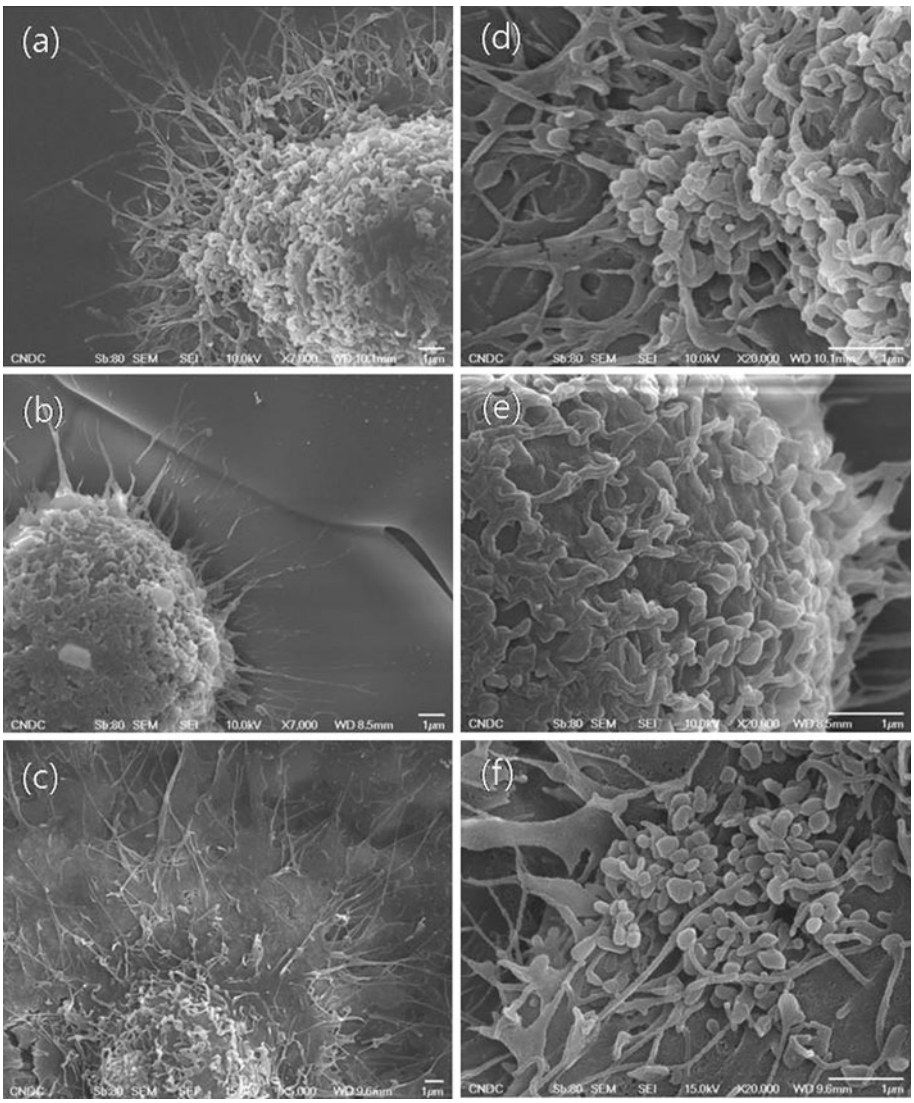

Fig. 4 SEM micrographs of MG-63 osteoblast cells on the surface of the **a**, **d** culture dish; **b**, **e** BCP and **c**, **f** silicon-doped BCP bone graft substitute 20 min after seeding. **d–f** Enlarged images of **a–c**

trypsin harvested cells on the surfaces of culture dishes (Fig. 4a, d), BCP granules without Si doping (Fig. 4b, e) and BCP granule with Si doping (Fig. 4c, f). However, after 20 min of layering, cellular morphology, filopodial growth and cytoplasmic webbing was different depending on the surfaces used. These cells had overall rough, round surfaces and microvilli-like projections.

According to Rajaraman et al. [42], cellular adhesion and spreading occurs through four events; attachment, filopodial growth, cytoplasmic webbing and flattening of the central mass. Rajaraman showed those 20 min after seeding, the cells entered into the fourth stages, although 70.8% cells were still in the advanced stage of cytoplasmic webbing [42]. However, it is worth noting that cytoplasmic webbing could progressively increase the contact area, thereby, making the cell-surface interaction more stable and stronger [43, 44].

The cells seeded on the culture plate belonged to the active filopodial growth stage as shown in Fig. 4a, d. The cells had active filopodial activity. The cells grown on the BCP granule surfaces were in the early stages of filopodial growth, i.e., filopodia had started to grow outside the cells, which is an early event of cellular attachment and spreading (Fig. 4b, e). However, cells grown on the silicon-doped BCP bone graft substitute (Fig. 4c, f), which were also in the early stage of cytoplasmic webbing, had more active filopodia that grew out of all sides of the cells. These extensive filopodia with cytoplasmic webbing on Si-doped BCP granule caused the cells to flatten [42]. In addition, under these conditions, the lamellipodia were grown out and were being filled with cytoplasma.

Figure 5 shows (a–c) MG-63 human osteoblast-like cells grown on the BCP bone graft substitutes and (b–d) silicon-doped BCP bone graft substitutes. The cells were well grown, had spread uniformly and the entire surface of the biomaterials were extensively covered with cells within 1 week. The cells migrated from the surface of the bone graft to the inside surface of the channel (c, f) and covered

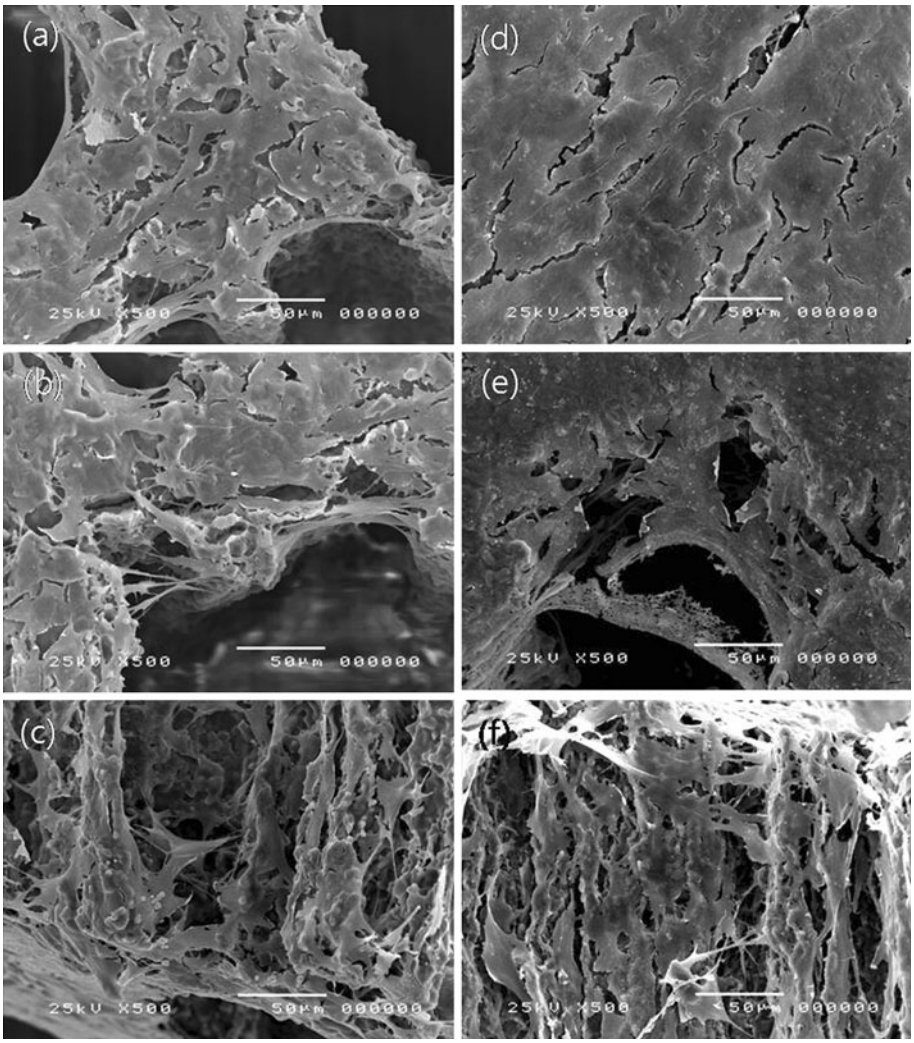

Fig. 5 SEM micrographs of MG-63 osteoblast cells on the surface of the BCP (**a**–**c**) and silicon-doped BCP (**d**–**f**)

the lumen (b, e). Pore size and porosity also play important roles in successful implantation, since these parameters dictate the space that will be available for cells to grow and the amount of oxygen and nutrients that will be supplied to the newly grown cells [45]. However, in this study both granule samples had the sample porosity and pore diameter and orientation, even though more abundant cellular growth was observed on the Si-doped BCP granules than the non-doped BCP granules (Fig. 5d–f).

3.4 Cellular differentiation

Upon the findings with cellular morphologies by SEM, we hypothesized that fast osteoblastic differentiation occurred on the Si-doped BCP granule. To verify this hypothesis, we used conditioned media to stimulate the cells for 7 and 14 days, which were then stained with alizarin red S and observed under a light microscope. Differentiation is very important in terms of bone remodeling. For bone formation processes and osteoclast resorption, preosteoblast cells or osteoprogenitor cells must go under cellular differentiation processes to become mature [46]. Mature osteoblast cells maintain a red color after Alizarin red S staining; thus, maturation can be notified by visualization under a light microscope. Figure 6 shows the differentiation of MG-63 cells on the control substrate (Fig. 6a, c), BCP granules without Si (Fig. 6b, e) and BCP granules with Si doping (Fig. 6c, f). Figure 6 clearly indicates that a higher rate of cellular differentiation occurs on the Si-doped bone substitutes. At day 14, cellular differentiation was greater than that of day 7, which also indicates that MG-63 cells readily proliferate on BCP granules doped with Si. The cellular differentiation on the BCP granules containing Si was even better than the positive control. These data also support the results obtained for MG-63 cellular proliferation; MG-63 cells proliferated up to 100% on the Si-doped BCP granules. Therefore, we believe that doping BCP with Si might result in improved osteoinduction, which will greatly help osteoblast cells differentiate and proliferate actively into culture vessels.

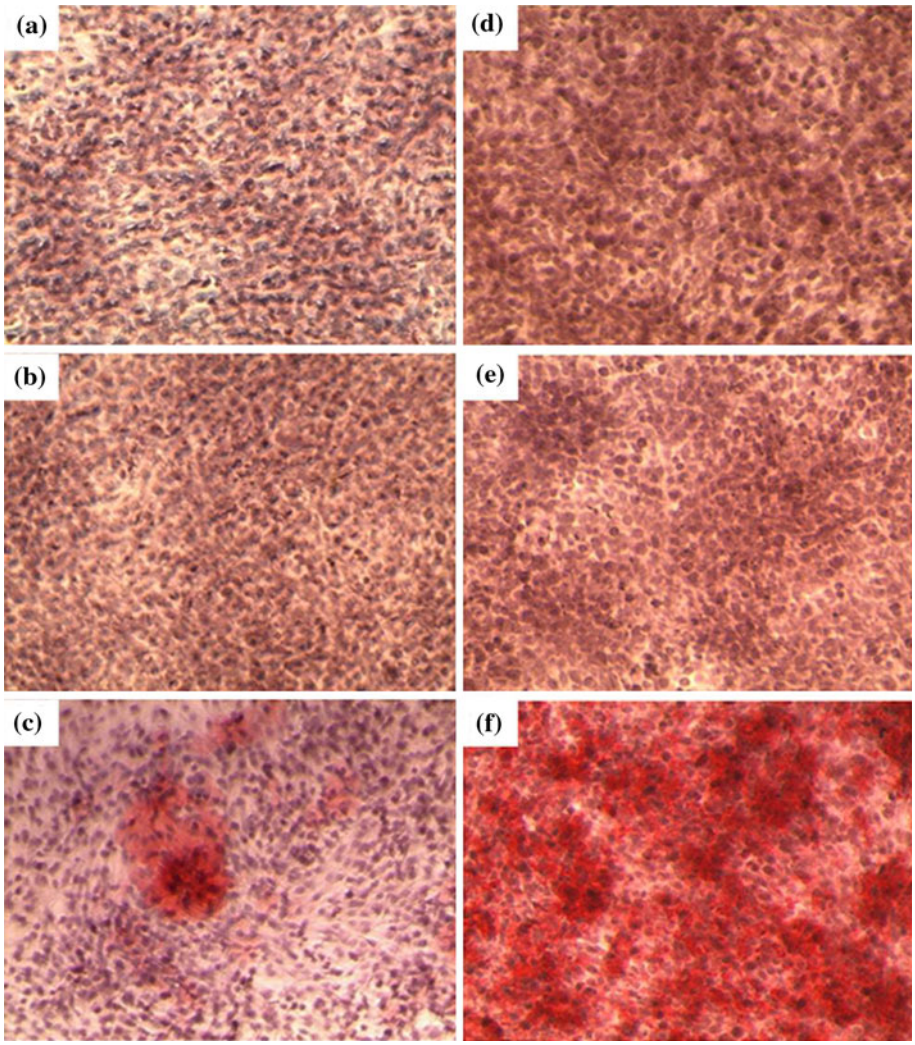

Fig. 6 Optical images of the differentiated MG-63 osteoblast-like cells at 7 (**a**–**c**) and 14 (**d**–**f**) days (**a**, **d**—control; **b**, **e**—BCP; **c**, **f**—Si-doped BCP)

However, it is worthy mentioning that the mechanism behind the high proliferation and differentiation of cells on Si-doped BCP was not characterized in this study. Several previous studies have also observed an increase in the growth of osteoblast-like cells upon Si doping of HA [41, 47]. It was assumed that the high dissolution of Si from the Ca phosphate compounds in physio-chemical environment might have a biologic effect on MG-63 cells due to the release of Si ions [24]. However, the mechanism behind the active growth proliferation of osteoblast-like cells upon Si-doping/substitution is not yet well understood [48]. According to Bohner, there is no current concrete experimental evidence that Si ions are released from Si-substituted calcium phosphates at therapeutic concentrations.

3.5 Gene expression

Apart from the controversy associated with Si dissolution, we also found that Si doping into BCP granules had a profound effect on the expression of various osteoblastic genes, which were time dependent. Figure 7 shows the variable expression ratios of osteonectin, osteopontin and collagen-1 at different time periods (day 3, 7 and 14). Bone is composed of inorganic compounds (hydroxyapatite and beta-tricalcium phosphate, etc.) and organic compounds (collagen complex, etc.). Especially, the ECM (extracellular matrix) is composed of several molecular complexes of proteins in bone and mediates cell adhesion to biomaterials [49]. Collagenous protein is the major ECM protein. Non-collagenous proteins are the second major ECM components including osteonectin, osteopontin, osteocalcin, etc. These proteins, such as osteonectin, osteopontin, are secreted in osteoblast and used as osteoblastic markers [50]. In this study, it appeared that although osteonectin and osteopontin were expressed during the early stage of cell differentiation, proliferation and attachment, the expression level of these genes only significantly increased at the intermediate (7 days) and late stages (14 days) (Fig. 7a, b). At day 3, the expression of the collagen type I gene was high in cells grown on Si-doped BCP. This gene was further over expressed at day 7 and then gradually decreased at day 14 (Fig. 7c). However, in comparison with control and non-doped BCP granule, gene expression level of collagen type I, osteonectin and osteopontin in Si-doped BCP granule increased significantly at day 14 ($P < 0.05$) (Fig. 7).

Collagen type I accounts for 90% of the total matrix organic component in bone, and provides bone with sufficient biomechanical strength. The mRAN level for type I collagen was highly expressed at differentiation day 3 (Fig. 7c).Therefore, in this study, it was evident that at the early stage of osteogenesis the silicon-doped BCP bone

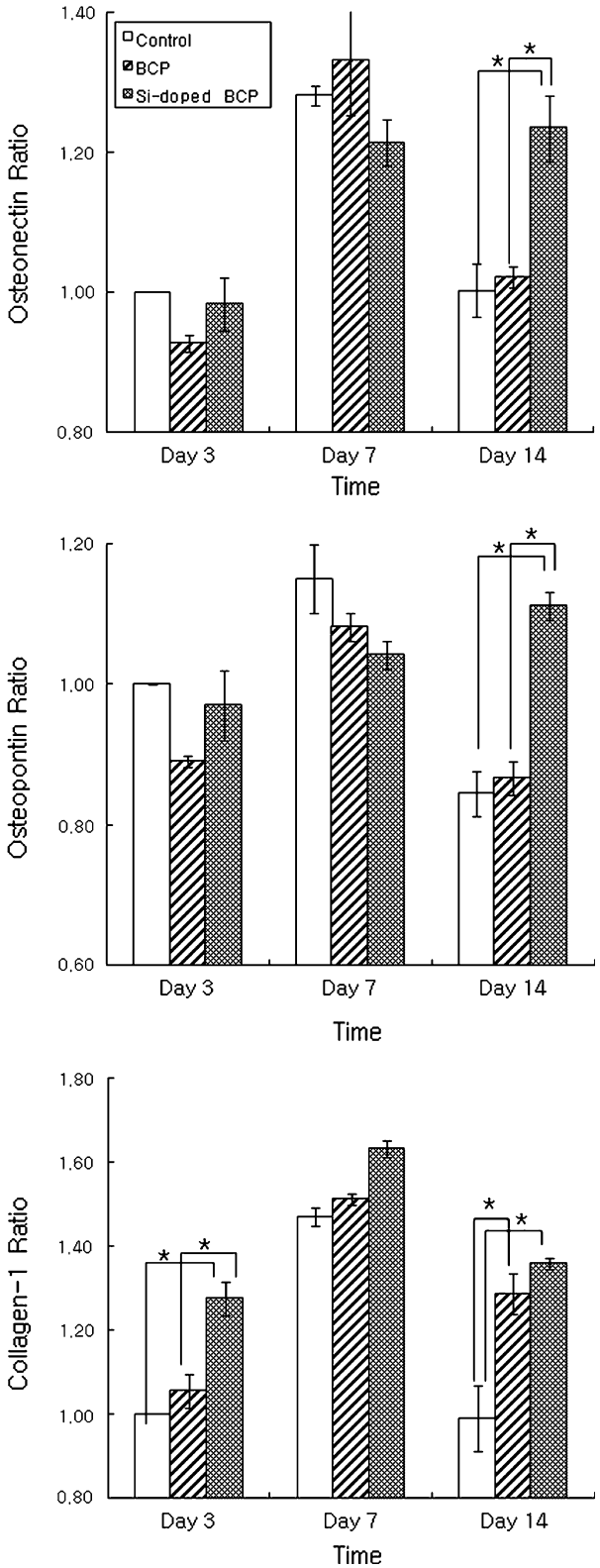

Fig. 7 Osteonectin, osteopontin and type 1 collagen gene expression in MG-63 osteoblast like cells. Cells were harvested after 3, 7, and 14 days and the mRNA levels of these genes were detected using RT-PCR. * Denotes the significant difference in the gene expression level ($P < 0.05$)

substitutes induced Type I collagen expression, whereas at the intermediate and late stage, osteonectin and osteopontin mRNA expression were induced. Through these gene regulations, silicon-doped BCP bone substitutes more quickly increased cell proliferation and differentiation.

4 Conclusion

The granule type, porous silicon-doped and non-doped BCP bone substitutes were successfully prepared using the Ultrasonic method and FM process. The granule type silicon-doped BCP showed no cytotoxicity with fibroblast-like cells L-929. Silicon-doped BCP enhanced MG-63 human osteoblast-like cell proliferation activity and differentiation. The cells on the surface of the silicon-doped BCP were well attached and spread. RT-PCR results showed that at day 14 of differentiation, the level of osteonectin and osteopontin mRNA expression were higher on Si-doped BCP than on the other surfaces. However, still the mechanism of these processes are not clear, but somehow silicon-doped BCP bone graft substitutes act like an enhancer or activator of osteoblastic cells. The biologic effects of silicon-doped BCP bone graft substitutes on MG-63 cells observed in this study might be related to an active mechanism by which Si doping may affect the topography of the BCP surface or through a passive mechanism by which fast dissolution of Si ion are released into an in vitro vessel. However, further studies are required regarding this issue. Detailed insight can be obtained by the quantitative analysis of the Si ion dissolution profile. Moreover, we still need to investigate the mechanisms by which silicon-doped BCP bone graft alter gene/protein-expression. In addition, we need to assess the osteoinduction ability and biodegradability of this bone substitute in animal models. Finally, these results suggest that the granular type silicon-doped BCP bone substitutes may be useful candidates in bone implant applications.

References

1. Hench LL. Biomaterials: a forecast for the future. Biomaterials. 1998;19:1419–23.
2. Oonishi H. Orthopaedic applications of hydroxyapatite. Biomaterials. 1991;12:171–8.
3. Yang S, Leong K-F, Du Z, Chua C-K. The design of scaffolds for use in tissue engineering. Part I. Traditional factors. Tissue Eng. 2001;7:679–89.
4. Chu T-MG, Orton DG, Hollister SJ, Feinberg SE, Halloran JW. Mechanical and in vivo performance of hydroxyapatite implants with controlled architectures. Biomaterials. 2002;23:1283–93.
5. Mastrogiacoma M, Muraglia A, Komlev V, Peryin F, Rustichelli F, Crovace A, et al. Tissue engineering of bone: search for a better scaffold. Orthodont Craniofac Res. 2005;8:277–84.
6. Dorozhkin SV, Epple M. Biological and medical significance of calcium phosphates. Angew Chem Int Ed. 2002;41:3130–46.
7. Buma P, Van Loon PJM, Versleyen H, Weinans H, Slooff TJJH, De Groot K, et al. Histological and biomechanical analysis of bone and interface reactions around hydroxyapatite-coated intramedullary implants of different stiffness: a pilot study on the goat. Biomaterials. 1997;18:1251–60.
8. Van Landuyt P, Li F, Keustermans JP, Streydio JM, Delannay F, Munting E. The influence of high sintering temperatures on the mechanical properties of hydroxylapatite. J Mater Sci: Mater Med. 1995;6:8–13.
9. Ripamonti U. Osteoinduction in porous hydroxyapatite implanted in heterotopic sites of different animal models. Biomaterials. 1996;17:31–5.
10. Gauthier O, Goyenvalle E, Bouler JM, Guicheus J, Pilet P, Weiss P, et al. Macroporous biphasic calcium phosphate ceramics versus injectable bone substitute: a comparative study 3 and 8 weeks after implantation in rabbit bone. J Mater Sci: Mater Med. 2001;12:385–90.
11. Yuan H, Yang Z, Bruijn JD, Groot K, Zhang X. Material-dependent bone induction by calcium phosphate ceramics: a 2.5-year study in dog. Biomaterials. 2001;22:2617–23.
12. Piattelli A, Scarano A, Mangano C. Clinical and histologic aspects of biphasic calcium phosphate ceramic (BCP) used in connection with implant placement. Biomaterials. 1996;17:1767–70.
13. Daculsi G. Biphasic calcium phosphate concept applied to artificial bone, implant coating and injectable bone substitute. Biomaterials. 1998;19:1473–8.
14. Elliot J. Structure and chemistry of the apatites and other calcium orthophosphates. New York: Elsevier; 1994.
15. Gibson IR, Best SM, Bonfield W. Chemical characterization of silicon-substituted hydroxyapatite. J Biomed Mater Res. 1999;44:422–8.
16. Carlisle EM. Silicon: a possible factor in bone calcification. Science. 1970;167:279–80.
17. Carlisle EM. A silicon requirement for normal skull formation in chicks. J Nutr. 1980;110(2):352–9.
18. Carlisle EM. Biochemical and morphological changes associated with long bone abnormalities in silicon deficiency. J Nutr. 1980;110:1046–56.
19. Alexandra EP. Nanoscale characterization of the interface between bone and hydroxyapatite implants and the effect of silicon on bone apposition. Micron. 2006;37:681–8.
20. Gao T, Aro HT, Ylänen H, Vuorio E. Silica-based bioactive glasses modulate expression of bone morphogenetic protein-2 mRNA in Saos-2 osteoblasts in vitro. Biomaterials. 2001;22:1475–83.
21. Reffitt DM, Ogston N, Jugdoahsingh R, Cheung HFJ, Evans BAJ, Thompson RPH, et al. Orthosilicic acid stimulates collagen type 1 synthesis and osteoblastic differentiation in human osteoblast-like cells in vitro. Bone. 2003;32:127–35.
22. Arumugam MQ, Ireland DC, Brooks RA, Rushton N, Bonfield W. Orthosilicic acid increases collagen type I mRNA expression in human bone-derived osteoblasts in vitro. Key Eng Mater. 2004;254:869–72.
23. Ni S, Chang J, Chou L, Zhai W. Comparison of osteoblast-like cell responses to calcium silicate and tricalcium phosphate ceramics in vitro. J Biomed Mater Res. 2006;80B:174–83.
24. Patel N, Best SM, Bonfield W. A comparative study on the in vivo behavior of hydroxyapatite and silicon substituted hydroxyapatite granules. J Biomed Mater Res. 2002;69:1199–206.
25. Patel N, Brooks RA, Clarke MT, Lee PMT, Rushton N, Gibson IR, et al. In vivo assessment of hydroxyapatite and silicate-substituted hydroxyapatite granules using an ovine defect model. J Biomed Mater Res. 2005;16:429–40.

26. Hing KA, Revell PA, Smith N, Buckland T. Effect of silicon level on rate, quality and progression of bone healing within silicate-substituted porous hydroxyapatite scaffolds. Biomaterials. 2006;27:5014–26.
27. Porter AE, Patel N, Skepper JN, Best SM, Bonfield W. Comparison of in vivo dissolution processes in hydroxyapatite and silicon substituted hydroxyapatite bioceramics. Biomaterials. 2003;24:4609–20.
28. Botelho CM, Lopes MA, Gibson IR, Best SM, Santos JD. Structural analysis of Si-substituted hydroxyapatite: zeta potential and X-ray photoelectron spectroscopy. J Mater Sci: Mater Med. 2002;13:1123–7.
29. Balas F, Perez-Pariente J, Vallet-Regi M. In vivo bioactivity of silicon substituted hydroxyapatites. J Biomed Mater Res. 2003;66A:364–75.
30. Popovic' D, Halloran JW, Hilmas GE, Brady GA, Somas S, Barda A, Zywicki G, Process for preparing textured ceramic composites, U.S. Patent 5645781.1997.
31. Baskaran S, Nunn S, Popovic' D, Halloran JW. Fibrous monolithic ceramics: I, fabrication, microstructure and indentation behavior. J Am Ceram Soc. 1993;76:2209–16.
32. Lee B-T, Sarkar SK, Song H-Y. Microstructure and material properties of double-network type fibrous (Al_2O_3–m-ZrO_2)/t-ZrO_2 composites. J Eur Ceram Soc. 2008;28:229–33.
33. Mickisch G, Fajta S, Keilhauer G, Schlick E, Tschada R, Alken P. Chemosensitivity testing of primary human renal cell carcinoma by a tetrazolium based microculture assay (MTT). Urol Res. 1990;18:131–6.
34. International standard 1999. Biological evaluation of medical devices. Part 5: Test for in vitro cytotoxicity. ISO-10993-5;1999 (E).
35. Patel N, Brooks RA, Clarke MT, Lee PMT, Rushton N, Gibson IR, et al. In vivo assessment of hydroxyapatite and silicate-substituted granules using an ovine model. J Mater Sci: Mater Med. 2005;16:429–40.
36. Hott M, Noel B, Bernache-Assolant D, Rey C, Marie PJ. Proliferation and differentiation of human trabecular osteoblastic cells on hydroxyapatite. J Biomed Mater Res. 1997;37:508–16.
37. Pioletti DP, Muller J, Rakotomanana LR. Effect of micromechanical stimulations on osteoblasts: development of a device simulating the mechanical situation at the bone-implant interface. Biomechanics. 2003;36:131–5.
38. Nanci A, Wuest JD, Peru L, Brunet P, Sharma V, Zalzal S, et al. Chemical modification of titanium surfaces for covalent attachment of biological molecules. J Biomed Mater Res. 1998;40:324–35.
39. Webb K, Hlady V, Tresco PA. Relationships among cell attachment, spreading, cytoskeletal organization, and migration rate for anchorage-dependent cells on model surfaces. J Biomed Mater Res. 2000;49:362–8.
40. Bigerelle M, Anselme K, Dufresne E. An unscaled parameter to measure the order of surfaces: a new surface elaboration to increase cells adhesion. Biomol Eng. 2002;19:79–83.
41. Xu L, Khor KA. Chemical analysis of silica doped hydroxyapatite biomaterials consolidated by a spark plasma sintering method. J Inorg Biochem. 2007;101:187–95.
42. Rajaraman R, Rounds DE, Yen SPS, Rembaum A. A scanning electron microscope study of cell adhesion and spreading in vitro. Exp Cell Res. 1974;88:327–39.
43. Grinnell F, Milam M, Srere PA. Studies on cell adhesion. III. Adhesion of baby hamster kidney cells. J Cell Biol. 1973;56:659.
44. Taylor AC. Attachment and spreading of cells in culture. Exp Cell Res. 1961;8:154–73.
45. Lajeunesse D, Frondoza C, Schoffield B, Sacktor B. Osteocalcin secretion by the human osteosarcoma cell line MG63. J Bone Miner Res. 1990;5:915–22.
46. Kartsogiannis V, Ng KW. Cell lines and primary cell cultures in the study of bone cell biology. Mol Cell Endocrinol. 2004;228:79–102.
47. Thian ES, Huang J, Best SM, Barber ZH, Bonefield W. Magnetron co-sputtered silicon-containing hydroxyapatite thin films—an in vitro study. Biomaterials. 2005;26(16):2947–56.
48. Bohner M. Silicon-substituted calcium phosphates—a critical view. Biomaterials. 2009;30:6403–6.
49. Deluca PP, Schrier JA. Recombinant human bone morphogenetic protein-2 binding and incorporation in PLGA microsphere delivery systems. Pharm Dev Technol. 1999;4:611–21.
50. De la Piedra GC, Jiménez RT. Usefulness of bone remodelling biochemical markers in the diagnosis and follow-up of Paget's bone disease, primary hyperparathyroidism, tumor hypercalcemia, and postmenopausal osteoporosis. II. Bone resorption markers. An Med Intern. 1990;7:534–8.